Mon. Not. R. Astron. Soc. **353,** 589–600 (2004) doi:10.1111/j.1365-2966.2004.08088.x

Planetary nebula distances re-examined: an improved statistical scale

J. P. Phillips★

Instituto de Astronomía y Meteorología, Av. Vallarta No. 2602, Col. Arcos Vallarta, C.P. 44130 Guadalajara, Jalisco, México

Accepted 2004 May 31. Received 2004 May 27; in original form 2003 November 26

ABSTRACT

The distances of planetary nebulae (PNe) are still quite uncertain. Although observational estimates are available for a small proportion of PNe, based on statistical parallax and the like, such distances are very poorly determined for the majority of galactic PNe. In particular, estimates of so-called 'statistical' distance appear to differ by factors of ∼2.7.

We point out that there is a well-defined correlation between the 5-GHz luminosity of the sources, L_5, and their brightness temperatures, T_B. This represents a different trend to those investigated in previous statistical analyses, and permits us to determine independent distances to a further 449 outflows. These distances are shown to be closely comparable to those determined using a T_B–R correlation, providing that the latter trend is taken to be non-linear.

This non-linearity in the T_B–R plane has not been noted in previous analyses, and is likely responsible for the broad (and conflicting) ranges of distance that have previously been published.

Finally, we point out that there is a close accord between observed trends within the L_5–T_B and T_B–R planes, and the variation predicted through nebular evolutionary modelling. This is used to suggest that observational biases are probably modest, and that our revised distance scale is reasonably trustworthy.

Key words: ISM: jets and outflows – planetary nebulae: general.

1 INTRODUCTION

The distances D of planetary nebulae (PNe) have been determined using a variety of observational procedures, although errors in these values are usually quite large. Apart from measures of trigonometric parallax [the most reliable of the procedures – see for instance Harris et al. (1997), Acker et al. (1998) and Gutierrez-Moreno et al. (1999)], such estimates have also been made using kinematic parallax (e.g. Liller & Liller 1968; Hajian, Terzian & Bignell 1993; Hajian & Terzian 1996; Reed et al. 1999), radial velocities (Acker 1978; Phillips 2001), spectroscopic parallax (Mendez & Niemela 1981; Ciardullo et al. 1999), trends in nebular extinction (e.g. Kaler & Lutz 1983; Gathier, Pottasch & Pel 1986; Martin 1994), values of Na D line absorption (Napiwotzki & Schönberner 1995), and determinations of central star gravities (e.g. Mendez et al. 1988; Mendez, Kudritzki & Herrero 1992).

It is possible to apply such procedures to only a small proportion of galactic PNe, however, and this has stimulated the attempt to develop further means of measuring D.

The earliest of these so-called 'statistical' procedures appears to be that of Shklovsky (Minkowski & Aller 1954), whereby nebular ionized masses were taken to be constant. It is clear, however, that such an assumption is based on shaky foundations, and it is more likely that ionized masses increase with radius (Pottasch 1980; Maciel & Pottasch 1980).

Further statistical procedures have been suggested by Minkowski (Aller 1965), Vorontsov-Veljaminov (1950) and Acker (1978), whereby compact PNe are taken to be optically thick, and assumed to have constant absolute visual luminosities. Daub (1982) and Cahn, Kaler & Stanghellini (1992) have used relations between ionized mass and shell optical depth, whilst Zhang (1995) and others have investigated the correlation between radio brightness temperature and radius. A fundamental challenge for all such analyses is to develop reliable lists of standard sources – of nebulae, that is, whose distances are well known. Zhang (1995), for instance, has developed a data base of 134 standard nebulae, and used these to investigate the distances of a further 515 PNe. However, the Zhang distances appear greatly to exceed values determined using statistical parallaxes, and other more or less direct observational procedures (Ciardullo et al. 1999; Gutierrez-Moreno et al. 1999; Napiwotzki 2001). Given that the latter measures of distance are likely to be reliable, this suggests that the standard distances of Zhang must be in error.

Phillips (2002a) has recently investigated this problem afresh, using a data list of known distances that is both highly selective and based upon the most reliable current measurements. Most of

★E-mail: jpp@cencar.udg.mx

these nebulae are located within 1 kpc of the Sun. He finds that mean nebular distances $\langle D \rangle$ are ∼37 per cent of those determined by Zhang (1995), and ∼51 per cent of those of Cahn et al. (1992).

It is therefore clear that many uncertainties remain concerning the true distances to these nebulae, and that systematic uncertainties in D may exceed ∼100 per cent.

These doubts have considerable repercussions for our understanding of the characteristics of these outflows. The masses of the nebulae, for instance, are exceedingly ill determined, depending as they do upon D^3. Similarly, uncertainties in D feed through to the estimation of nebular formation rates (e.g. Pottasch 1996; Phillips 2002a) and galactic chemical gradients (Maciel 2000).

Various further attempts have therefore been made to investigate which of these differing methods may be the most appropriate – larger scales such as that of Zhang (1995), or the shorter distances of Phillips (2002a), Daub (1982) and Cahn et al. (1992). These appear, for the most part, to favour the larger distance estimates. Thus Phillips (2001) has shown that the Zhang (1995) and van de Steene & Zijlstra (1995) scales are consistent with galactic trends in radial velocity. Similarly, Cudworth (1974) and Phillips (2004) derive comparable distances using mean statistical parallaxes, and the angular dimensions of Type I outflows.

We would like, in the following analysis, to outline a further way in which mean distance scales may be assessed. We shall find that PNe occupy a fairly narrow regime within the 5-GHz luminosity–brightness temperature plane. This permits us to define mean trends between these parameters, and to evaluate distances to a further 449 nebulae. It will be shown that the observed trend for the standard sources of Zhang (1995) and Phillips (2002a) is consistent with evolutionary expectations, and implies a mean distance scale that is ∼0.83 times that of Zhang (1995).

2 OBSERVED AND EXPECTED VARIATION OF LUMINOSITY WITH BRIGHTNESS TEMPERATURE

The stellar evolutionary models of Schönberner (1979, 1981, 1983) and Blocker & Schönberner (1990) have been used to estimate the variation of the 5-GHz luminosity L_5 with brightness temperature T_B, where

$$L_5 = F_{\rm obs}(5\,{\rm GHz/mJy})(D/{\rm kpc})^2,$$

and $F_{\rm obs}$(5 GHz/mJy) is the observed flux at 5 GHz. It follows that L_5 is proportional to the intrinsic 5-GHz flux. We shall assume that the central stars follow hydrogen-burning tracks within the HR plane (Henry & Shipman 1986; Schönberner 1989). Similarly, the nebulae will be assumed to become optically thin to H ionizing radiation shortly after the termination of central star hydrogen burning, at the point at which luminosity is dominated by gravo-thermal energy release (e.g. Schönberner 1993). In fact, the precise point at which shells become optically thin is still poorly determined, although a somewhat earlier or later onset makes little difference to our results. The fit to observed sources is relatively insensitive to this parameter.

The evolution of shell ionization-front velocities V_i is quite uncertain. Certain models predict shell acceleration (e.g. Okorokov et al. 1985; Schmidt-Voigt & Köppen 1987; Mellema 1994; Marigo et al. 2001), whilst others favour either invariant velocities (e.g. Okorokov et al. 1985) or shell deceleration (Ferch & Salpeter 1975). Some of these models are more sophisticated and complete than others, although it is clear that much depends upon uncertain analytical assumptions, and the values that are adopted for the shell physical characteristics. We shall, in the present analysis, adopt the variation of V_i with R_i determined by Marigo et al. (2001). This appears typical of the more reliable (and recent) of these models. We shall also assume that shell velocities take a value of 25 km s^{-1} at the onset of optically thin expansion, consistent with expansion velocities for a wide variety of PNe (Phillips 2002b).

Finally, we note that the ionized radius R_i at any particular time $T_{\rm ev}$ depends upon the so-called transition period $T_{\rm tran}$, which is the time between when the central stars leave the asymptotic giant branch (AGB) and an observable PNe is formed. This value does not appear to be correlated with the mass of the central star (Vassiliadis & Wood 1994), but may be dependent upon the phase of the pulse cycle at which the star leaves the AGB (Vassiliadis & Wood 1994). We shall assume a value $T_{\rm tran} = 1.5 \times 10^3$ yr consistent with various of the models of Marigo et al. (2002). A larger value than this would shift our model trajectories to lower values of T_B.

The results of our analysis are indicated in Fig. 1. Dotted segments of the curves correspond to phases of rapid nebular evolution, and are associated with a low incidence of PNe. The 'grey' sections of curves correspond to phases of optically thin expansion. Filled circles correspond to the standard sources of Zhang (1995), whilst open circles are associated with those of Phillips (2002a). Only a few nebulae are common to the two standard source lists, and we have preferred (for these cases) to use the distances of Phillips (2002a). The trend for the central star mass $M_{\rm cs} = 0.546$ M$_\odot$ assumes envelopes to be optically thick during central star hydrogen burning, as is the case for nebulae having higher central star masses. Whether this is the case is far from clear, although it is unlikely that many PNe are associated with such low-mass star.

The model evolutionary tracks appear in agreement with the observed distribution of standard sources. In particular, the incidence of sources having high T_B and low L_5 is small, as would be expected given the rapid evolution of L_5 within this regime. Similarly, the fall-off of L_5 with T_B is as would be expected for optically thin expansion, providing that central star masses take a value $M_{\rm cs} \geqslant 0.57$ M$_\odot$. The apparent absence of lower $M_{\rm cs}$ sources is consistent with our current understanding of central star mass functions (e.g. Weidemann 1989; Kaler & Jacoby 1991; Zhang & Kwok 1993).

Finally, we note that the maximum predicted values of L_5, which occur in a regime $1 < \log(T_B/{\rm K}) < 4$, are consistent with the values determined for the Zhang (1995) standard sources. This is of particular interest from the point of view of the present analysis, since such estimates depend upon the maximum luminosities and temperatures of the central stars alone; the values of L_5(peak) are not dependent upon shell characteristics, apart from requiring that PNe are optically thick to H I ionizing radiation. This agreement therefore represents strong evidence that our standard source distances are (for the most part) correct. Similarly, the agreement between observations and models, extending over some eight orders of magnitude in T_B, is suggestive that observed trends are reasonably reliable. Biases arising from source selection effects are likely to be relatively modest.

This does not, however, apply for the individual standard source listings. The Zhang (1995) sources, for instance, are concentrated towards higher values of T_B. This is broadly as would be expected given that they are at larger distances from the Sun, and interstellar extinction reduces the detectability of lower surface brightness shells. What is much less expected, however, is paucity of brighter nebulae in the listing of Phillips (2002a). The nebulae in this subset are located within 1 kpc of the Sun, and should constitute a more representative sample than is the case with Zhang (1995). This is clearly not the case. Such a paucity of higher-luminosity nebulae

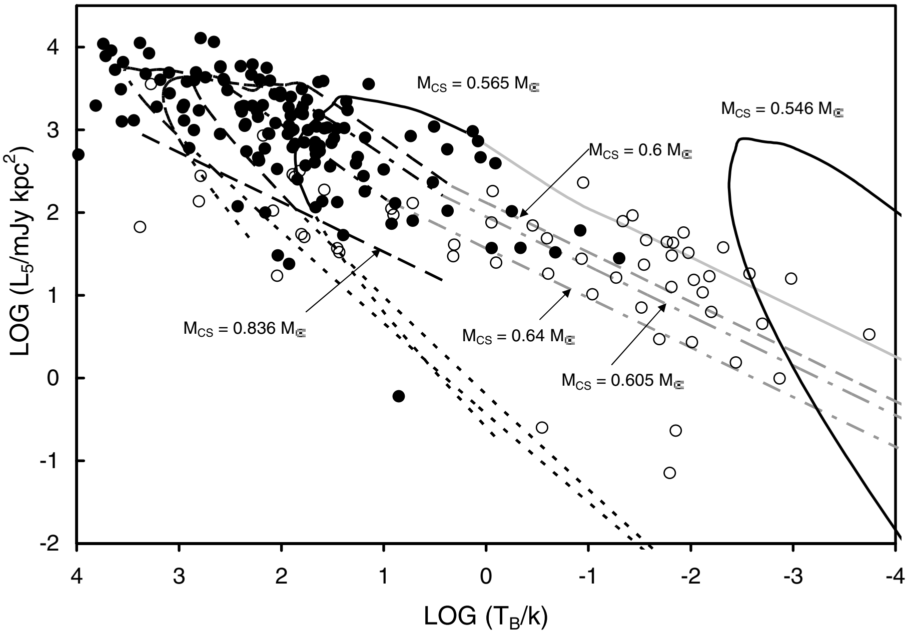

Figure 1. The distribution of theoretical tracks and standard sources within the L_5–T_B plane. The filled circles correspond to the standard sources of Zhang (1995), and open circles to the sources of Phillips (2002a), whilst the curves represent predictions for differing central star masses. Note that the dotted segments of the tracks (towards lower values of L_5) correspond to phases of rapid PNe evolution, during which the observed incidence of nebulae is predicted to be low. The 'grey' sections of curve represent phases of optically thin expansion.

has also been noted in the local sample of Pottasch (1996), and presumably implies that certain higher-luminosity sources are closer than is currently appreciated.

It would seem likely that these differing biases contribute to the varying distance scales noted in Section 1 (see the discussion in Section 4). Fortunately, both sets of bias are complementary, and we shall later concatenate these results to obtain improved distance estimates.

Similar modelling may also be undertaken for the T_B–R planes of Zhang (1995), or the M_i–τ planes of Cahn et al. (1992) and Daub (1982). Our results show comparable levels of agreement, as may be noted from the trends illustrated in Fig. 2. It should be emphasized, on the other hand, that deduced values of T_B depend upon the evolution of both central stars and shells; there are no regimes (as for L_5) where one or other of these strands predominates. The agreement with observations therefore depends upon the (still uncertain) characteristics of shell expansion.

Finally, it is apparent that the distribution of sources within the L_5–T_B plane is reasonably well defined, and is at least as good as those for the T_B–R plane of Zhang (1995), or the M_i–τ planes of Daub (1982), Cahn et al. (1992) and others. It is therefore of interest to determine what scale of distances such a correlation would imply.

3 MEAN DISTANCE SCALE

The distribution of the Zhang (1995) and Phillips (2002a) sources is further illustrated in Fig. 3, together with the least-squares trend

$$\log\left(\frac{F_5}{\text{mJy kpc}^2}\right) = 0.4337 \log\left(\frac{T_B}{K}\right) + 2.0388 \qquad (1)$$

calculated on the assumption that the primary errors occur in the vertical axis. Uncertainties in distance are probably of the order of $\Delta D/D \cong 0.35$, although errors are likely to be somewhat lower for the sources of Phillips (2002a), and larger for those of Zhang (1995). Such errors lead to vertical displacements in source position, such as is indicated by the arrow in Fig. 3.

Two important points may be noted with respect to this uncertainty in D. The first is that the size of the arrow is significantly smaller than the scatter in the results, suggesting that the intrinsic distribution of sources is comparable to that which is observed. Errors in T_B are likely to be of the order of $\Delta\log(T_B) \sim 0.15$, and therefore contribute relatively little to the observed scatter. The second is that the arrow is, by and large, perpendicular to the least-squares trend. Such errors are therefore unlikely to affect least-squares gradients to any appreciable degree.

The scatter of these results about the least-squares trend implies a typical uncertainty in D of the order of $\sigma(D) \sim 0.18$ kpc.

Four of the sources (Th 2-A, He 1-5, HW 5 and HW 6) lie outside of the primary nebular sequence, and have not been used in assessing the least-squares trend. They are indicated by crosses in Fig. 3. The placement of at least two of these nebulae (Th 2-A and He 1-5) suggests that they may be rapidly evolving towards higher values of L_5 (see Fig. 1).

We have used equation (1) to recalculate distances to a further 449 sources, using the values of brightness temperature summarized by Zhang (1995). The sources are constrained to the longitude range $10° \leqslant l \leqslant 350°$, thereby eliminating most bulge PNe. Our values of D are summarized in Table 1, together with the comparative values of Phillips (2002a) and Zhang (1995). A comparison between our present results and those of Zhang (1995) is also illustrated in Fig. 4.

Finally, it is interesting to ask what distances the T_B–R correlation might imply, and how these compare with those of the L_5–T_B correlation. If one again concatenates the two groups of standard distances, those of Phillips (2002a) and Zhang (1995), then one obtains a distribution that extends over a much larger range of the T_B axis, as noted in Fig. 2. It is apparent, from this enhanced data set, that there is evidence for a turnover in the trend of T_B with R. Gradients d $\log(T_B)$/d $\log(R)$ are lower where $\log(R/\text{pc}) < -1$. A

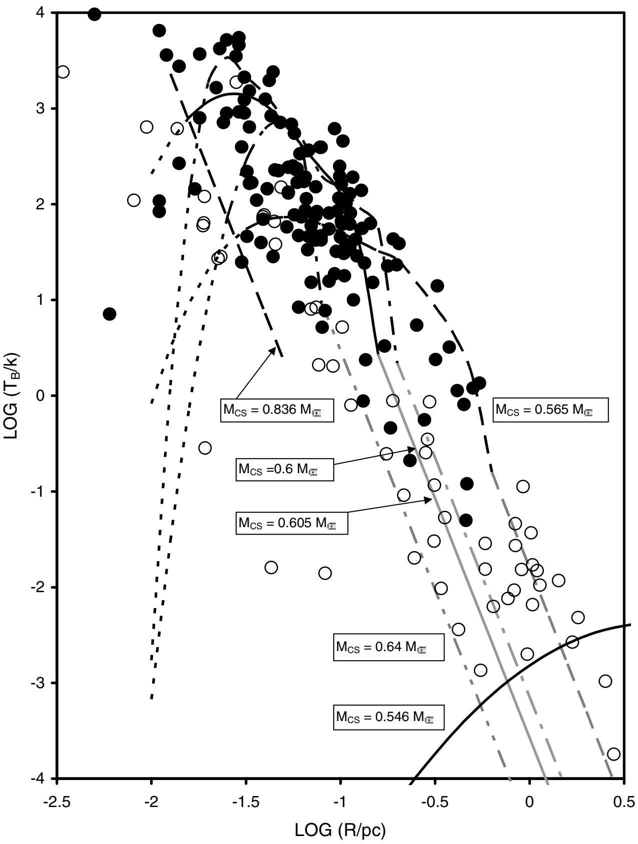

Figure 2. Variation of 5-GHz brightness temperatures T_B with nebular radius R for the standard sources of Zhang (1995) (•) and Phillips (2002a) (○), as well as for the models of nebular evolution discussed in the text. The various models are labelled according to central star mass M_{cs}. Dotted curves refer to periods of rapid evolution, when the incidence of nebulae is expected to be low, 'grey' curves correspond to optically thin expansion, whilst 'black' curves represent phases of expansion during which shells are expected to be optically thick.

second-order least-squares polynomial fit yields the relation

$$\log\left(\frac{R}{\mathrm{pc}}\right) = -2.12\times10^{-3}\left[\log\left(\frac{T_{\mathrm{B}}}{\mathrm{K}}\right)\right]^2 - 0.281\log\left(\frac{T_{\mathrm{B}}}{\mathrm{K}}\right) - 0.665. \qquad (2)$$

One may compare the distances determined through this equation with those evaluated through the (linear) L_5–T_{B} correlation. Specifically, if one defines a scaling factor

$$\kappa(L_5\text{–}T_{\mathrm{B}} \mid R\text{–}T_{\mathrm{B}}) = \frac{\langle D(L_5\text{–}T_{\mathrm{B}})\rangle}{\langle D(R\text{–}T_B)\rangle} \equiv \frac{\sum_{i=1}^{N} D_{\mathrm{i}}(L_5\text{–}T_{\mathrm{B}})}{\sum_{i=1}^{N} D_{\mathrm{i}}(R\text{–}T_{\mathrm{B}})}, \qquad (3)$$

where values $D_i(L_5$–$T_{\mathrm{B}})$ are determined in the L_5–T_{B} plane, and $D_i(R$ –$T_{\mathrm{B}})$ using equation (2), then one finds

$\kappa(L_5\text{–}T_{\mathrm{B}} \mid R\text{–}T_{\mathrm{B}}) = 1.079 \pm 0.054.$

Whilst the combinations of parameters are therefore quite different, the L_5–T_{B} and T_{B}–R correlations appear to be in accord when it comes to determining relative distance scales. It also appears that individual distances $D_i(R$ –$T_{\mathrm{B}})$ and $D_i(L_5$–$T_{\mathrm{B}})$ are in very close accord.

We therefore conclude that the L_5–T_{B} correlation represents a useful alternative method for testing mean distances to the PNe. Not only is the correlation different from those used in previous analyses, but the procedure is open to direct comparison with stellar evolutionary theory. Peak values of L_5 are found to be consistent with what is expected from central star evolution. In addition, the entire range of variation in L_5 appears consistent with models of central star and nebular evolution. The distances are therefore likely to have a fair chance of being reliable.

This scale also appears consistent with the results of a revised analysis in the T_{B}–R plane, in which both groupings of standard sources are again concatenated.

Finally, it should noted that the L_5–T_{B} trends are open to a variety of potential biases. Thus, errors in D for more distant nebulae tend to be larger than for sources located closer to the Sun. This may have a disproportionate influence upon least-squares fits, and affect the distribution of brighter sources in particular. It also appears that some of the gravity distances of Zhang (1995) may be subject to strong systematic errors (e.g. Zhang 1993; Phillips 2002a).

Low surface brightness nebulae are often difficult to detect as distances become larger, partly as a result of increasing levels of interstellar extinction. Similarly, younger, higher surface brightness outflows may be difficult to identify as a result of their small angular dimensions. These and other factors mean that the sample of PNe is neither complete nor representative, and may give a misleading impression of luminosity trends.

Values of T_{B} have been assessed using measures of 5-GHz radio fluxes S(5 GHz), and source angular sizes θ. These latter values are mainly based upon radio interferometric results, although they also contain a small admixture of optical estimates as well. The values of T_{B} therefore correspond to means over the projected shell surfaces. It is probable that the primary error in these temperatures derives from uncertainties in θ. These errors may arise from the presence of multiple shell structures, the variation of optical size with ionic transition, the differing levels at which contours are measured, and so forth. A detailed discussion of these effects is to be found in Bensby & Lundstrom (2001). Most of these errors will simply lead to increased scatter within the L_5–T_{B} and T_{B}–R planes. However, there is also the possibility that such uncertainties may result in systematic biases as well. In particular, smaller, more compact, sources are likely to have sizes that are less reliable than is the case for larger outflows. This may lead to an overestimate of θ (and an underestimate of T_{B}) where radii R are small, and some decrease in gradients d log(T_{B})/d log(R).

Finally, and as noted above, the Zhang (1995) and Phillips (2002a) sources have deficits of low and high T_{B} sources. This is compensated for in the present analysis by concatenating the two distance sets.

Our results are therefore by no means free from bias, and there is certainly room for improvement. In particular, the deficit of brighter local PNe is somewhat troubling, certain of the less reliable 'standard' distances might very well be pruned, and the overall corpus of known distances might usefully be increased. Attempts should also, where possible, be made to improve the balance of the sample, so as to include appropriate proportions of differing nebular types and surface brightnesses.

Having said all this, the agreement between model and observed trends (discussed in Section 2) is such as to instill a reasonable level of confidence in our deduced correlations. Biases are unlikely to cause appreciable distortion within the L_5–T_{B} and T_{B}–R planes.

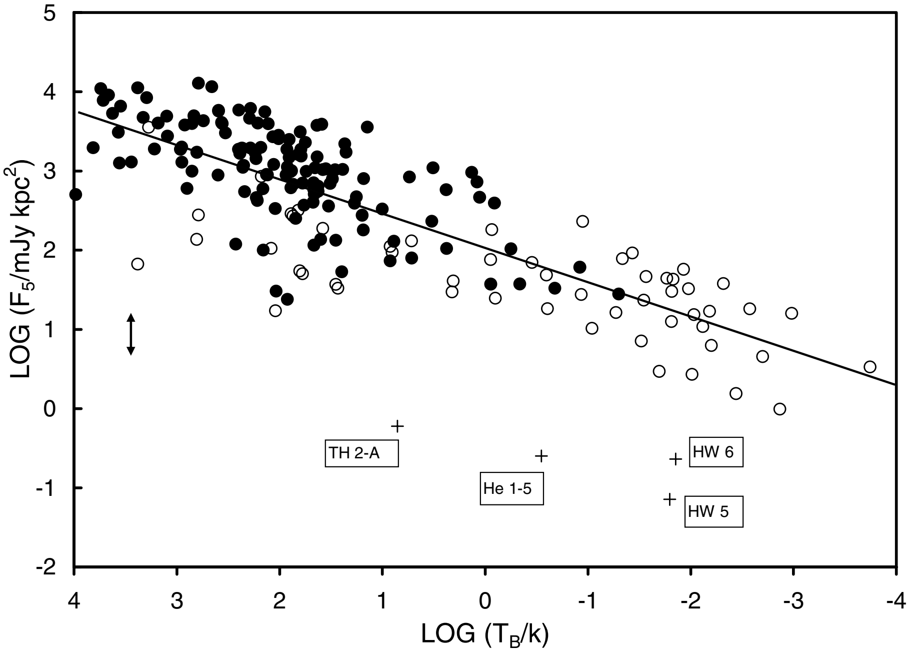

Figure 3. The distribution of the standard sources of Zhang (1995) and Phillips (2002a) within the L_5–T_B plane, where the line corresponds to a least-squares fit. The vertical arrow represents the displacement to be expected where source distances are in error by a factor $\Delta D/D = 0.35$. Note that the four sources marked by crosses (+) fall outside of the main PNe sequence, and have not been used in calculating the least-squares relation.

Table 1. Distances to galactic planetary nebulae.

Name	PG	*D*(Phillips) (kpc)	*D*(Zhang) (kpc)	*D*(Present) (kpc)
NGC 6537	10+00 1	0.59	1.62	1.77
M 2-17	10+04 1	2.80	7.47	5.57
M 2-9	10+18 1	1.13	3.01	1.82
NGC 6578	10−01 1	0.92	2.47	2.31
IC 4732	10−06 1	1.82	4.92	4.79
Pe 1-13	10−06 2	4.56	12.17	8.29
M 1-32	11+04 1	1.37	3.68	3.17
NGC 6439	11+05 1	1.74	4.71	4.64
M 2-15	11+06 1	2.61	6.98	5.37
M 2-13	11+11 1	3.82	10.38	10.68
NGC 6567	11−00 2	0.94	2.54	2.40
M 1-47	11−05 1	2.70	7.22	5.95
H 2-48	11−09 1	1.98	5.45	6.23
M 1-45	12−02 1	2.87	7.73	7.43
M 1-33	13+04 1	1.71	4.62	4.63
Sn 1	13+32 1	4.07	10.91	9.42
M 1-48	13−03 1	3.72	9.93	7.57
VV 3-4	13−04 1	5.40	14.64	14.65
M 1-50	14−04 1	1.66	4.47	4.12
VV 3-6	14−05 2	4.66	12.72	13.72
M 1-31	14−07 1	4.98	13.6	14.79
M 1-39	15+03 1	1.39	3.78	3.92
A 44	15−03 1	1.73	4.71	2.38
M 1-53	15−04 1	1.60	4.3	3.93
M 1-46	16−01 1	1.15	3.08	2.58
M 1-54	16−04 1	1.50	4.01	3.09
M 1-56	16−04 2	3.19	8.71	9.48
M 1-52	17−02 1	3.05	8.13	5.93
M 3-30	17−04 1	2.50	6.71	3.97
A 51	17−10 1	1.23	3.34	1.77
A 65	17−21 1	2.00	5.86	2.28
M 4-8	18+03 1	3.43	9.37	10.21
M 3-52	18+04 1	4.00	10.7	6.57

Table 1 – *continued*

Name	PG	*D*(Phillips) (kpc)	*D*(Zhang) (kpc)	*D*(Present) (kpc)
Na 1	18+20 1	1.92	5.14	4.20
M 3-54	18−02 1	3.32	8.87	6.92
M 3-25	19+03 1	2.03	5.65	6.89
M 4-10 1	19−02 1	2.84	7.83	9.04
M 1-60	19−04 1	2.04	5.55	5.81
M 1-61	19−05 1	1.71	4.73	5.59
A 66	19−23 1	0.60	1.68	0.73
Sa 1-8	20−05 1	2.95	7.87	6.33
M 3-28	21−00 1	2.00	5.37	4.87
M 1-51	21−01 1	0.65	1.74	1.59
M 1-63	21−05 1	3.25	8.71	7.32
M 1-57	22−02 1	1.34	3.6	3.21
M 1-58	22−03 1	1.50	4.04	3.69
K 3-11	23−01 1	2.91	7.84	7.33
M 1-59	23−02 1	1.29	3.5	3.54
M 2-40	24+03 1	1.96	5.24	4.67
M 4-9	24+05 1	1.06	2.83	1.72
M 2-46	24−02 1	2.93	7.84	6.48
Pe1-17	24−03 1	3.64	9.72	7.29
IC 4593	25+40 1	1.08	2.89	2.42
Pe 1-15	25−02 1	3.45	9.22	7.40
IC 1295	25−04 1	0.85	2.28	1.18
A 60	25−11 1	1.57	4.26	2.07
NGC 6818	25−17 1	0.63	1.68	1.47
Pe 2-15	26−01 2	3.84	10.31	9.34
Pe 1-19	26−02 3	3.95	10.56	8.42
M 2-45	27+00 1	1.01	2.73	2.64
M 2-43	27+04 1	1.32	3.74	5.00
Pe 1-18	27−02 1	2.59	7.17	8.44
Vy 1-4	27−03 2	2.46	6.62	6.01
IC 4846	27−09 1	2.07	5.61	5.72
M 2-44	28+01 1	1.48	3.97	3.45
K 3-7	28+02 1	1.96	5.25	4.52

Table 1 – *continued*

Name	PG	*D*(Phillips) (kpc)	*D*(Zhang) (kpc)	*D*(Present) (kpc)
K 3-2	28+05 1	2.36	6.39	6.37
Pe 1-21	28−03 1	1.82	4.85	3.95
Pe 1-20	28−04 1	1.97	5.27	4.52
NGC 6751	29−05 1	1.10	2.94	2.18
K 3-6	30+04 1	2.79	7.42	10.20
K 3-3	31+05 1	1.63	4.35	3.43
M 3-34	31−10 1	1.87	5	4.12
K 3-11	32+07 1	4.08	10.89	8.31
PC 19	32+07 2	2.55	6.89	6.75
M 1-66	32−02 1	1.87	5.09	5.39
K 3-18	32−03 1	4.61	12.64	13.98
NGC 6741	33−02 1	0.86	2.33	2.32
A 55	33−05 1	2.21	5.94	2.98
NGC 6772	33−06 1	0.73	1.96	1.11
K 3-13	34+02 1	2.13	5.74	5.50
M 1-33	34+04 1	1.71	4.62	4.63
K 3-5	34+06 1	4.18	11.17	7.11
NGC 6572	34+11 1	0.38	1.02	1.06
NGC 6778	34−06 1	1.24	3.31	2.54
Ap 2-1	35−00 1	0.54	1.43	1.13
Sh 2-71	36−01 1	0.73	1.97	1.05
NGC 6790	37−06 1	1.13	3.18	4.10
CN 3-1	38+12 1	1.50	4.05	4.00
A 70	38−25 1	1.74	4.69	2.58
K 3-7	39+02 1	0.74	1.99	2.04
M 2-47	39−02 1	1.70	4.57	4.12
A 53	40−00 1	0.89	2.38	1.68
K 3-30	40−03 1	2.54	6.84	6.46
NGC 6781	41−02 1	0.37	0.99	0.61
K 3-14	42+05 1	6.15	16.67	16.89
NGC 6807	42−06 1	3.29	9.16	11.18
NGC 6852	42−14 1	1.59	4.24	2.66
M 1-65	43+03 1	2.42	6.51	5.94
M 3-27	43+11 1	2.48	6.91	8.55
NGC 6210	43+37 1	0.64	1.73	1.55
M 4-14	43−03 1	3.15	8.4	6.28
A 67	43−13 1	1.90	5.25	2.45
K 3-33	45−01 1	3.73	10.21	11.33
VY2-2	45−02 1	2.65	7.93	9.82
NGC 6804	45−04 1	0.70	1.88	1.32
PB 9	46−03 1	1.61	4.31	3.57
NGC 6803	46−04 1	1.22	3.29	3.26
A 39	47+42 1	1.81	4.56	1.86
A 62	47−04 1	0.30	0.81	0.49
He 2-429	48+01 1	1.62	4.37	4.33
K 3-29	48+01 2	2.30	6.43	8.07
K 3-19	48+04 1	3.25	8.93	10.01
K 4-16	48+04 2	5.61	14.99	11.98
PB 10	48−02 1	1.53	4.08	3.53
He 2-428	49+02 1	3.20	8.55	6.16
M 1-67	50+03 1	0.43	1.14	0.69
K 4-28	50−01 1	4.15	11.56	14.27
He 2-430	51+03 1	2.42	6.64	7.36
M 1-73	51−03 1	1.73	4.65	4.17
K 3-31	52+02 2	2.52	6.93	7.83
K 3-41	52−02 1	10.78	29.34	30.60
Me 1-1	52−02 2	1.81	4.86	4.58
M 1-74	52−04 1	3.12	8.62	10.15
A 59	53+03 1	1.26	3.4	1.69
K 3-38	53−01 1	2.08	5.59	5.09
M 1-72	54−02 1	3.49	9.8	12.54
NGC 6891	54−12 1	1.03	2.76	2.35
He 2-432	55+02 1	2.45	6.65	6.88

Table 1 – *continued*

Name	PG	*D*(Phillips) (kpc)	*D*(Zhang) (kpc)	*D*(Present) (kpc)
He 2-433	55+02 2	2.47	6.58	5.06
He 2-435	55+02 3	2.74	7.32	6.25
A 54	55+06 1	2.86	8.07	3.48
A 46	55+16 1	2.17	5.99	2.74
He 2-439	55−00 1	1.15	3.17	3.68
K 3-35	56+02 1	2.08	5.73	6.56
K 3-42	56−00 1	3.50	9.58	10.57
NGC 6804	56−04 1	0.70	1.88	1.32
K 4-30	57+01 1	2.81	7.6	7.47
He 2-447	57−01 1	2.27	6.3	7.63
NGC 6879	57−08 1	2.52	6.74	5.78
K 3-40	58+01 1	2.55	6.86	6.18
IC 4997	58−10 1	1.59	4.43	5.45
K 3-37	59+02 1	3.05	8.22	7.93
K 3-39	59+02 2	4.50	12.29	13.35
A 72	59−18 1	1.19	3.25	1.47
He 2-440	60+01 1	2.22	6.04	6.45
K 4-39	60−02 1	4.09	11.03	10.46
NGC 6886	60−07 2	1.16	3.13	2.94
M 4-16	61+02 1	7.07	19.64	23.59
DDDM -1	61+41	5.65	15.35	15.85
NGC 6905	61−09 1	0.97	2.6	1.62
NGC 6765	62+09 1	1.54	4.14	2.41
M 2-48	62−00 1	2.77	7.46	7.00
K 3-48	63+00 1	1.89	5.07	4.46
K 3-54	63−06 1	5.49	15.01	16.39
BD+30	64+05 1	0.67	1.85	2.14
M 1-64	64+15 1	3.98	10.74	6.00
NGC 6058	64+48 1	2.09	5.63	3.34
K 3-53	64−02 1	2.45	6.95	9.27
NGC 6842	65+00 1	0.69	1.85	1.25
He 1-6	65−05 1	1.67	4.45	2.91
K 648	65−27 1	2.97	7.96	7.10
PC 24	66−05 1	2.52	6.74	5.78
NGC 7094	66−28 1	1.81	4.8	2.16
K 3-52	67−00 1	2.51	7.1	9.42
K 4-41	68+01 1	3.06	8.21	7.59
He 2-453	68+01 2	1.87	4.99	3.18
PC 23	68+03 1	2.94	7.96	8.06
M 1-75	68−00 1	1.70	4.53	3.32
He 2-459	68−02 1	2.17	6.02	7.24
K 3-55	69+00 1	1.21	3.26	2.96
K 3-49	69+02 1	9.32	22.49	34.50
NGC 6894	69−02 1	0.88	2.36	1.44
M 3-35	71−02 1	1.58	4.44	5.62
K 3-57	72+00 1	1.51	4.05	3.72
NGC 6881	74+02 1	1.44	3.96	4.48
A 69	76+01 1	2.88	7.75	4.42
K 3-77	78+00 1	1.94	5.18	4.28
A 50	78+18 1	4.90	13.56	6.25
A 78	81−14 1	1.95	5.38	2.22
NGC 6884	82+07 1	0.97	2.63	2.70
NGC 6833	82+11 1	3.66	10.13	12.09
NGC 6826	83+12 1	0.53	1.42	1.20
A 71	85+04 1	0.61	1.64	0.84
Hu 1-2	86−08 1	0.99	2.66	2.53
K 8-78	88+04 1	2.88	7.73	6.85
NGC 7048	88−01 1	1.01	2.7	1.50
NGC 7026	80+00 1	0.75	2.03	1.91
Sh 1-89	89−00 1	1.11	2.96	1.88
M 1-77	89−02 1	1.98	5.29	4.29
IC 5117	89−05 1	1.36	3.83	5.01
M 1-78	93+01 1	0.50	1.38	1.62

Table 1 – *continued*

Name	PG	*D*(Phillips) (kpc)	*D*(Zhang) (kpc)	*D*(Present) (kpc)
K 3-82	93−00 1	1.40	3.73	2.49
M 1-79	93−02 1	1.59	4.26	2.62
K 1-16	94+27 1	1.27	3.39	2.98
K 3-83	94−00 1	3.70	9.87	7.71
K 3-62	95+00 1	1.48	4.07	4.62
A 73	95+07 1	1.81	4.98	2.31
M 2-49	95−02 1	2.32	6.3	6.47
K 4-45	96+00 1	0.95	2.58	1.34
K 3-61	96+02 1	2.65	7.07	5.73
A 77	97+03 1	0.46	1.22	0.85
M 2-50	97−02 1	3.79	10.13	8.07
K 3-60	98+04 1	2.30	6.28	6.87
IC 5217	100−05 1	1.02	2.74	2.71
Me 2-2	100−08 1	2.64	7.3	8.56
A 75	101+08 1	1.42	3.82	2.04
A 79	102−02 1	1.29	3.48	1.93
A 80	102−05 1	2.22	6.4	2.43
M 2-51	103+00 1	1.12	2.99	1.88
M 2-52	103+00 1	2.15	5.74	3.97
BI 2-1	104+00 1	2.20	6.05	6.94
NGC 7139	104+07 1	1.08	2.92	1.56
M 2-53	104−01 1	2.16	5.77	3.64
M 2-54	104−06 1	5.07	13.81	14.61
NGC 7354	107+02 1	0.48	1.3	1.19
M 1-80	107−02 1	1.98	5.29	4.29
K 3-87	107−02 1	4.06	10.84	7.91
Vy 2-3	107−13 1	5.05	13.48	9.95
K 1-20	110−12 1	4.23	11.63	5.29
K 4-58	111+06 1	3.45	9.2	6.15
HB 12	111−02 1	2.88	8.11	10.46
A 84	112−10 1	1.48	4.28	1.74
A 82	114−04 1	1.98	5.55	2.41
M 2-55	116+08 1	1.48	3.98	2.31
IC 1454	117+18 1	4.23	11.63	5.29
Sh 1-118	118+02 1	1.11	3	1.43
Vy 1-1	118−08 1	2.19	5.87	4.98
BV 5-1	119+00 1	1.51	4.05	2.32
A 1	119+06 1	2.17	5.9	2.95
Hu 1-1	119−06 1	1.85	4.93	3.86
NGC 40	120+09 1	0.46	1.21	0.98
We 1-1	121+03 1	4.66	12.55	6.57
A 2	122−04 1	3.49	9.51	4.68
IC 3568	123+34 1	1.08	2.9	2.47
K 3-90	126+03 1	2.34	6.24	4.60
K 3-91	129+04 1	5.43	14.56	8.65
We 2-5	129−02 1	0.89	2.5	1.06
IC 1747	130+01 1	0.96	2.58	2.23
K 3-92	130+03 1	4.56	12.26	7.11
M 1-1	130−11 1	3.42	9.13	7.27
A 3	131+02 1	2.86	7.71	3.42
K 4-60	132−00 1	0.49	1.31	1.20
IC 289	138+02 1	0.63	1.68	1.18
A 5	141−07 1	2.47	6.63	2.53
K 3-94	142+03 1	3.32	8.87	5.98
NGC 1501	144+06 1	0.56	1.48	1.03
M 4-18	146+07 1	2.55	6.85	6.37
M 2-2	147+04 1	1.53	4.1	3.66
M 1-4	147−02 1	1.31	3.53	3.39
K 4-47	149+04 1	6.02	20.42	22.46
VV 1-2	151+02 1	0.34	0.94	0.48
Sh 2-207	151−02 1	0.35	0.95	0.53
A 16	153+22 1	1.73	4.99	1.90
A 28	158+37 1	1.18	4.28	1.21

Table 1 – *continued*

Name	PG	*D*(Phillips) (kpc)	*D*(Zhang) (kpc)	*D*(Present) (kpc)
IC 351	159−15 1	1.99	5.32	4.45
We 2	160−00 1	0.21	0.55	0.43
IC 2003	161−14 1	1.80	4.81	3.89
K 3-67	165−06 1	2.23	6.09	6.49
IC 2149	166+10 1	0.77	2.07	2.03
CRL 618	166−06 1	1.24	3.3	2.72
A 8	167−00 1	1.20	3.23	1.78
K 3-66	167−09 1	3.11	8.42	8.42
IC 2120	169−00 1	0.70	1.86	1.26
K 3-69	170+04 1	9.45	25.48	13.87
BA 1	171−25 1	1.73	4.66	2.63
A 9	172+00 1	4.09	11.41	5.05
H 3-29	174−14 1	1.86	4.98	3.40
Pu 1	181+01 1	1.93	5.24	2.49
Vy 1-1	181−08 1	2.00	5.34	4.60
M 1-5	184−02 1	1.81	4.96	5.49
M 1-7	189+07 1	2.35	6.26	4.50
NGC 2372-2	189+19 1	0.77	2.07	1.32
J 320	190−17 1	2.11	5.63	4.63
J 900	194+02 1	1.26	3.4	3.29
Sh 2-266	195−00 1	0.61	1.62	1.04
VV 1-5	196−01 1	0.20	0.53	0.30
NGC 2022	196−10 1	0.98	2.6	2.02
A 11	196−12 1	1.99	5.36	3.05
VV 1-4	197−02 1	0.31	0.84	0.54
A 14	197−03 1	2.66	7.25	3.77
K 1-7	197−14 1	3.63	9.84	4.71
A 12	198−06 1	1.20	3.21	2.04
A 19	200+08 1	2.57	6.88	3.06
K 4-48	201+02 1	3.38	9.13	8.86
A 13	204−08 1	1.59	4.13	1.74
YM 29	205+14 1	0.26	0.71	0.32
NGC 1535	206−40 1	0.80	2.14	1.77
A 30	208+33 1	2.48	6.97	2.55
M 1-80	210+01 1	1.67	4.45	3.06
M 1-6	211−03 1	1.59	4.35	4.70
M 1-9	212+04 1	2.61	7.08	7.22
A 20	214+07 1	1.93	5.25	2.50
IC 418	215−24 1	0.37	1.02	1.10
A 18	216−00 1	1.34	3.61	1.84
M 3-35	221+05 1	3.14	8.4	5.46
A 17	221−04 1	2.89	7.98	3.74
IC 2165	221−12 1	0.93	2.52	2.47
We 6	224+01 1	5.09	12.31	5.22
K 1-13	224+15 1	0.68	1.85	0.91
M 1-16	226+05 1	2.22	5.99	5.71
A 32	227+33 1	1.20	3.23	1.46
M 1-17	228+05 1	3.11	8.4	8.23
M 1-18	231+04 1	4.20	11.58	5.40
NGC 2438	231+04 2	0.78	2.09	1.20
M 1-13	232−01 1	2.27	6.07	4.51
M 1-11	232−04 1	1.54	4.24	4.90
A 15	233−16 1	1.46	3.91	2.38
NGC 2440	234+02 1	0.58	1.57	1.40
VV 1-7	235+01 1	0.61	1.72	0.75
M 1-14	235−01 1	1.62	4.37	4.23
M 1-12	235−03 1	2.37	6.48	7.13
K 1-12	236+03 1	1.92	5.18	2.86
Sa 2-21	238+07 1	3.19	8.83	4.11
A 33	238+34 1	1.18	2.92	1.21
NGC 2610	239+13 1	1.19	3.18	1.86
Sa 2-22	240+07 1	3.78	10.1	6.98
M 3-27	240−07 1	4.65	12.42	8.25

Table 1 – *continued*

Name	PG	*D*(Phillips) (kpc)	*D*(Zhang) (kpc)	*D*(Present) (kpc)
M 3-4	241+02 1	4.20	11.28	6.58
M 6-1	242−11 1	1.86	4.96	3.78
NGC 2452	243−01 1	1.17	3.11	2.31
M 3-5	245+01 1	2.89	7.72	5.90
A 34	248+29 1	1.09	2.91	1.12
M 4-2	248−08 1	2.36	6.3	5.26
A 23	249−05 1	2.05	5.51	2.74
A 26	250+00 1	3.19	8.83	4.11
K 1-21	251−01 1	2.65	7.16	3.88
K 1-1	252+04 1	1.77	4.78	2.59
M 3-6	254+05 1	1.21	3.24	2.74
H 1-32	255−02 3	2.78	7.69	9.09
He 2-9	258−00 1	1.06	2.88	3.11
He 2-11	259+00 1	0.40	1.07	0.77
He 2-15	261+02 1	0.92	2.46	1.92
NGC 2818	261+08 1	1.14	3.05	1.79
PB 2	263−05 1	2.11	5.71	5.75
He 2-7	264−08 1	1.39	3.7	2.91
He 2-5	264−12 1	2.38	6.43	6.30
NGC 2792	265+04 1	0.71	1.89	1.26
PB 3	269−03 1	1.39	3.73	3.40
He 2-35	274+02 2	2.42	6.48	5.61
He 2-37	274+03 1	1.59	4.24	2.80
He 2-28	275−02 1	2.04	5.44	4.15
He 2-29	275−02 2	1.75	4.68	3.41
He 2-25	275−03 1	0.61	1.7	2.07
PB 4	275−04 1	1.24	3.32	2.81
He 2-21	275−04 2	3.15	8.5	8.21
NGC 2899	277−03 1	0.69	1.84	1.06
PB 6	278+05 1	1.71	4.56	3.55
NGC 2867	278−05 1	0.71	1.9	1.69
He 2-26	278−06 1	1.13	3.03	1.91
IC 2501	281−05 1	1.15	3.21	4.03
My 60	283+02 1	1.45	3.89	3.47
K 1-22	283+02 5	1.34	3.43	1.47
He 2-50	283+03 1	2.43	6.49	4.54
Pe 1-1	285+01 1	1.37	3.75	4.16
IC 2553	285−05 1	1.18	3.17	2.85
NGC 3211	286−04 1	0.73	1.94	1.70
H 2-41	286−06 1	1.56	4.16	3.39
He 2-51	288−05 1	1.41	3.77	3.23
He 2-63	289+07 1	3.32	8.93	8.09
AG Car	289−00 1	0.51	1.36	1.07
Fg 1	290+07 1	1.09	2.91	2.02
IC 2621	291−04 1	1.02	2.79	2.94
IC 2501	291−05 1	0.79	2.12	2.09
NGC 3699	292+01 1	0.90	2.39	1.54
PB 8	292+04 1	2.16	5.79	5.15
NGC 3918	294+04 1	0.44	1.19	1.17
NGC 4361	294+43 1	0.46	1.25	0.74
He 2-73	296−03 1	1.54	4.18	4.23
NGC 3195	296−20 1	1.18	3.16	1.96
NGC 4071	298−04 1	1.17	3.17	1.73
He 2-85	300−01 1	1.06	2.84	2.53
He 2-86	300−02 1	1.31	3.58	3.85
IC 4191	304−04 1	0.83	2.23	1.95
Th 2-A	306−00 1	1.08	2.89	2.07
NGC 5189	307−03 1	0.33	0.88	0.55
MyCn 18	307−04 1	1.23	3.32	3.23
He 2-10	308−12 1	1.72	4.61	2.67
He 2-99	309−04 1	1.86	4.98	3.40
NGC 5315	309−04 2	0.72	1.96	2.14
He 2-10 13	310−02 1	1.79	4.78	3.17

Table 1 – *continued*

Name	PG	*D*(Phillips) (kpc)	*D*(Zhang) (kpc)	*D*(Present) (kpc)
He 2-10 12	311+02 1	1.73	4.63	3.77
NGC 5307	312+10 1	1.07	2.86	2.42
He 2-10	312−01 1	1.31	3.5	2.97
He 2-10	315+05 1	2.40	6.41	5.06
He 2-111	315−00 1	1.20	3.2	2.66
He 2-10	316+08 1	1.67	4.45	3.49
He 2-119	317−05 1	0.77	2.05	1.33
He 2-114	318−02 1	1.86	5.01	2.80
He 1-116	318−02 2	2.08	5.59	2.80
He 2-112	319+06 1	1.09	2.91	2.36
IC 4406	319+15 1	0.79	2.11	1.50
He 2-120	321+01 1	1.45	3.87	2.51
He 2-115	321+02 1	1.26	3.47	3.91
He 2-117	321+02 2	0.91	2.48	2.69
Pe 2-8	322−00 1	1.74	4.83	5.83
Mz 1	322−02 1	1.07	2.85	2.03
NGC 5979	322−05 1	1.11	2.97	2.77
He 2-123	323+02 1	1.30	3.52	3.59
He 2-132	323−02 1	1.62	4.33	3.02
He 2-164	323−03 1	1.00	2.67	2.17
He 2-125	324+02 1	2.72	7.33	6.96
He 2-133	324−01 1	1.05	2.88	3.18
NGC 6026	341+13 1	1.39	3.72	2.17
H 1-13	342+00 1	0.51	1.39	1.36
NGC 6072	342+10 1	0.57	1.53	0.98
Me 2-1	342+27 1	1.91	5.11	4.32
Sp 3	342−14 1	0.98	2.62	1.75
PC 17	343−07 1	2.72	7.27	6.12
He 2-175	345+06 1	2.02	5.41	4.58
K 1-32	346+12 1	0.26	0.69	0.51
He 2-129	325+03 1	2.59	7.09	7.85
He 2-141	325−04 1	1.32	3.53	2.77
IC 972	326+42 1	2.09	5.69	2.87
He 2-143	327−01 1	1.22	3.3	3.32
He 2-140	327−01 2	1.68	4.6	5.03
He 2-142	327−02 1	1.70	4.62	4.75
He 2-158	327−06 1	6.45	17.26	14.71
He 2-163	327−07 1	3.36	9.05	5.08
He 2-146	328−02 1	0.72	1.93	1.57
Sp 1	329+02 1	0.76	2.05	1.21
He 2-149	329−02 1	3.56	9.55	8.52
Mz 2	329−02 2	1.01	2.7	2.00
He 2-153	330−02 1	5.72	15.43	8.43
He 2-159	330−03 1	1.88	5	3.90
NGC 5873	331+16 1	1.71	4.58	4.23
Mz 3	331−01 1	0.44	1.17	1.03
He 2-157	331−02 1	2.35	6.35	6.24
He 2-161	331−02 2	1.71	4.56	3.64
He 2-165	331−03 2	1.50	4.04	2.20
He 2-164	332−03 1	1.00	2.67	2.17
He 2-152	333+01 1	0.84	2.26	2.09
IC 4642	334−09 1	1.21	3.23	2.52
He 2-169	335−01 1	1.07	2.88	2.70
Hf 2-1	335−04 1	2.79	7.44	5.33
Pe 1-6	336+01 1	1.70	4.56	3.94
He 2-186	336−05 1	2.69	7.25	6.90
PC 14	336−06 1	1.91	5.11	4.32
He 2-155	338+05 1	1.16	3.09	2.47
NGC 6326	338−08 1	1.22	3.26	2.71
K 1-32	340+12 1	2.57	6.99	3.16
NGC 6153	341+05 1	0.50	1.34	1.17
IC 4663	346−08 1	1.37	3.66	2.82
He 2-1781	347+05 1	2.47	6.96	9.01

Table 1 – *continued*

Name	PG	*D*(Phillips) (kpc)	*D*(Zhang) (kpc)	*D*(Present) (kpc)
IC 4669	348−13 1	2.24	5.99	4.91
NGC 6302	349+01 1	0.21	0.57	0.52
M 2-4	349+04 1	2.50	6.81	7.15
NGC 6337	349−01 1	0.75	2.01	1.33
H 2-1	350+04 1	1.94	5.31	5.84

Table 2. Relative distance scales for the sources listed in Table 1.

Comparative scale	*N*	κ(stat | pres)
Present work	449	1.000
Zhang (1995)	449	1.198 ± 0.060
van de Steene & Zijlstra (1995)	278	1.048 ± 0.066
Cahn et al. (1992)	439	0.885 ± 0.044
Daub (1982)	213	0.730 ± 0.041
Phillips (2002a)	449	0.396 ± 0.020

4 COMPARISON BETWEEN ALTERNATIVE DISTANCE SCALES

It is relevant, at this point of the discussion, to ask how well our present distances compare with those of previous analyses. One straightforward way of doing this would be to compare the relative distance scales κ (stat | pres) between prior distances *D*(stat) and those of our present analysis *D*(pres). This parameter is defined in the same way as for κ (L_5–T_B | R –T_B) (see Section 3 and equation 3), and applies for all of the sources listed in Table 1. Values of κ(stat | pres) are summarized in Table 2 for the statistical distances of Daub (1982), Cahn et al. (1992), Zhang (1995), Phillips (2002a), and van de Steene & Zijlstra (1994).

It is plain that our present distance scale is most similar to those of Zhang (1995), Cahn et al. (1992) and van de Steene & Zijlstra (1994), whilst that of Phillips (2002a) appears to be the most disparate. Most of these sources correspond to higher T_B outflows, however, and these global differences conceal a more interesting story.

One may also define a scaling factor κ (stat | stand) for the standard sources alone, again similar to the parameter κ (L_5–T_B | R–T_B) defined above. One is, in this case, evaluating the mean ratio between previous statistical distances *D*(stat), and the standard source distances *D*(stand) employed here. Note, however, that many of our lower brightness temperature standards are not included in prior listings of statistical distance. We have therefore determined new values of *D*(stat) where this proved necessary, using the correlations between T_B, θ, M_i and D specified in previous analyses. Thus, Zhang (1995) determines a median trend

$$\log(D/\mathrm{kpc}) = 1.603 - 0.5805\log(\theta) - 0.155\log(T_B) - 0.2095\log[F_{\mathrm{obs}}(5\,\mathrm{GHz})]. \quad (4)$$

We have used this relation, together with the values of θ and F_{obs}(5 GHz) quoted by Phillips (2002a) and Zhang (1995), to evaluate equivalent 'Zhang' distances *D*(stat) for sources having $\log(T_B) < -0.5$. The only instance where this procedure could not be implemented was in the case of Acker (1978), where distances were determined using a variety of procedures.

The relevant values of κ(stat | stand) are indicated in Table 3, where we have indicated the values to be expected for the entire corpus of standard sources (κ_{all}(stat | stand)), and for those having brightness temperatures $\log(T_B) < -0.5$ [i.e. κ_{low}(stat | stand)], and $\log(T_B) > -0.5$ [i.e. κ_{high}(stat | stand)]. The values *N* correspond to the total sample numbers.

It may be seen that the distances of Daub (1982) and Acker (1978) appear to be too low, irrespective of the range of T_B that is considered. Other scales are much less consistent, however. The scales of Cahn et al. (1992), Zhang (1995), van de Steene & Zijlstra (1994), Schneider & Buckley (1996) and Bensby & Lundstrom (2001) appear quite reasonable where $\log(T_B) > -0.5$, for

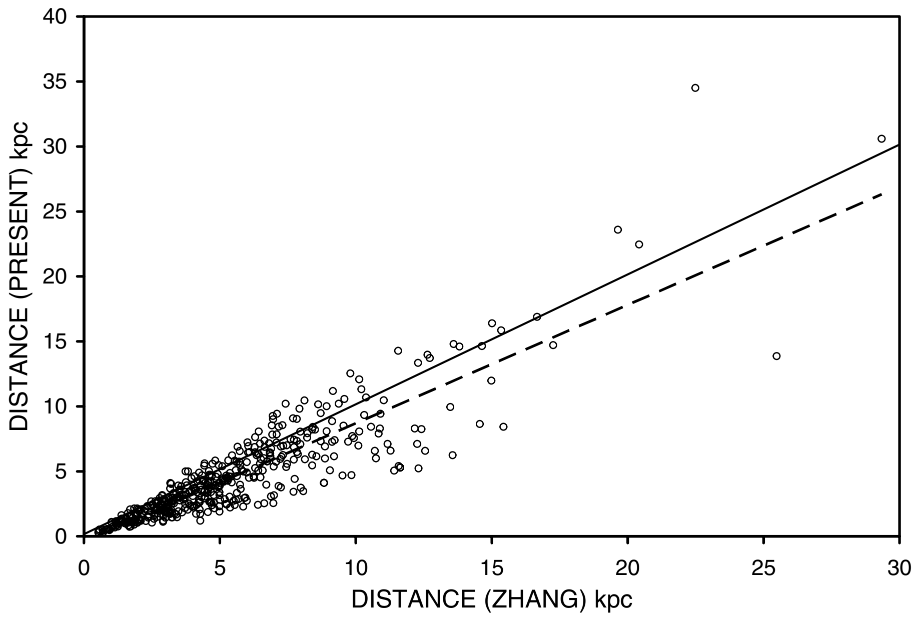

Figure 4. A comparison between distances determined using the present L_5–T_B correlation, and those determined by Zhang (1995). The solid line corresponds to a one-to-one relation, whilst the dashed line represents a least-squares fit. It will be noted that both of these trends are similar, implying similar mean scales of PNe distance.

Table 3. Relative distance scales for standard sources.

Comparative scale	N	κ_{all}(stat | stand)	N	κ_{low}(stat | stand)	N	κ_{high}(stat | stand)
Present work	172	0.889 ± 0.086	31	1.068 ± 0.177	141	0.884 ± 0.079
Zhang (1995)	172	1.022 ± 0.093	31	2.525 ± 0.416	141	0.982 ± 0.085
van de Steene & Zijlstra (1995)	172	0.947 ± 0.087	31	2.059 ± 0.339	141	0.916 ± 0.079
Phillips (2002a)	172	0.369 ± 0.033	31	1.004 ± 0.166	141	0.352 ± 0.030
Cahn et al. (1992)	172	0.792 ± 0.079	31	0.736 ± 0.177	141	0.793 ± 0.073
Daub (1982)	172	0.573 ± 0.057	31	0.748 ± 0.127	141	0.568 ± 0.053
Acker (1978)	109	0.672 ± 0.078	11	0.833 ± 0.281	98	0.667 ± 0.076
Bensby & Lundstrom (2001)	172	1.000 ± 0.090	31	3.060 ± 0.506	141	0.945 ± 0.081
Schneider & Buckley (1996)	172	0.910 ± 0.088	31	0.637 ± 0.112	141	0.917 ± 0.081

instance, although all of these are poorer when it comes to representing lower T_B sources. By contrast, the correlation of Phillips (2002a) is extremely good at determining distances to lower T_B outflows, but appears to fail completely when it comes to sources at higher T_B.

Finally, our present distances show the least variation in κ(stat | stand) of any of these scales, and can be used with a reasonable level of confidence at both high (and particularly) lower values of T_B. It appears to be the only scale having such a broad range of applicability. An alternative methodology might be to use the results of Zhang (1995) or Bensby & Lundstrom (2001) for higher T_B outflows, and those of Phillips (2002a) for PNe having $\log(T_B) < -0.5$. Although our scaling factors are calculated solely for the L_5–T_B correlation, essentially identical results are determined for the T_B–R correlation as well.

Where brightness temperatures are large, then the present correlations yield values of D that are slightly too low (by $\sim$10 per cent). This probably reflects the broad scatter of high T_B sources with respect to L_5, and the fact that our least-squares fits are made in the logarithmic plane.

The close correspondence between standard source distances and our present scale is hardly surprising, given that the self-same standards were used to define this scale in the first place. However, the improvement noted here is also a consequence of the enhanced data base that we have employed, a feature that represents one of the primary advances of our present analysis. This also enables us to avoid several of the confusions that have arisen in previous studies, as will be explained in more detail in the following section.

Finally, we note that the scaling factor κ(stat | stand) is only one of many parameters that can be used to compare distances. Such a scale is also open to bias, in the sense that values of κ are dominated by trends at larger distances D. The results of an alternative (logarithmic) comparison are described in the Appendix. This will confirm the results described above, and indicates an even closer agreement between standard distances and our estimates $D(L_5$–$T_B)$ in Table 1.

5 WHY DO PRESENT DISTANCES DIFFER FROM THOSE OF PREVIOUS STATISTICAL STUDIES?

It is pertinent to ask why our present results differ from those of previous statistical analyses. In particular, why should analyses of trends between T_B and R lead to such markedly differing results?

One reason for such disparities may reside in the increasing numbers of sources located at 'known' distances, as measures of parallaxes, central star gravities and so forth are determined for increasing numbers of outflows. It is also likely that the accuracy of many of these distances is increasing with time. Both of these factors should permit us to determine improved correlations between T_B and R.

A further important (and possibly related) reason concerns the quality of the supposed correlations. Cahn et al. (1992) determine the relation between ionized mass M_i and a parameter τ (related to the nebular optical depth), for instance. It can be shown that such an analysis is essentially identical to those within the T_B–R plane (e.g. Zhang 1995; Bensby & Lundstrom 2001; Phillips 2002a).

The scatter in the Cahn et al. (1992) results is appreciable, however, and their deduced correlation requires the eye of faith. Similar problems appear to plague most other M_i–τ analyses, and are probably responsible for the large ranges of gradient $d\log(M_i)/d\log(\tau)$ noted by Kwok (1985).

Finally, we note that the present analysis reveals a further source of error. It has been pointed out that the T_B–R relation is non-linear, a trend that is predicted from our evolutionary modelling, and is confirmed through the distribution of our standard sources. It follows that gradients $d\log(T_B)/d\log(R)$ will differ between high and low brightness temperature sources.

This change in gradient was *not* noted in previous analyses because of the limited ranges of T_B over which they applied. The analysis of Zhang (1995), for instance, applies for predominantly higher temperature sources, and his trends can only be applied where $\log(T_B) > 0$. The results of Phillips (2002a) were biased towards lower temperature sources, and his correlation is inappropriate where values of T_B are large.

The combination of the non-linearity between T_B and R, and differing ranges of standard source brightness temperatures, therefore leads to strong biases between the respective distance scales.

The analysis of these scales undertaken in Section 4 broadly confirms these expected differences. The statistical distances of Zhang (1995) are probably more accurate where values of T_B are large, whilst those of Phillips (2002a) are most applicable where values of T_B are low.

The present results, on the other hand, appear to show reasonable levels of accuracy at all values of T_B.

6 CONCLUSIONS

The distances of PNe are for the most part uncertain. There is a relative paucity of values based upon direct observational measures, and those which are known are associated with appreciable levels of uncertainty. Whilst statistical distances have been determined for larger numbers of PNe, these appear to be prone to substantial systematic biases. Differing estimates of distance appear to vary by factors of ~2.7.

We have used the correlation between 5-GHz brightness temperatures T_B, and intrinsic radio luminosities L_5 to undertake a further investigation of the distances to PNe.

A comparison between trends expected from models of nebular evolution, and the standard sources of Zhang (1995) and Phillips (2002a), indicates a close similarity between the peak luminosities L_5(peak). Similarly, observed trends within the L_5–T_B plane appear closely similar to those determined through nebular modelling, an agreement that extends over some eight orders of magnitude in T_B. This accord between theory and observations suggests that our standard source distances are likely to be tolerably correct. It also implies that the distributions of sources are relatively unaffected by bias.

We note that sources at known distance occupy relatively narrow ranges of the L_5–T_B plane. We have therefore used this correlation to estimate distances to a further 449 nebulae. The results imply mean distances $\langle D \rangle$ that are significantly greater than those of Phillips (by a factor ~2.2), and somewhat less than those of Zhang (by a factor 0.83 ± 0.04). This result is also confirmed through a reanalysis of the T_B–R correlation, in which the distribution of sources is fitted using a least-squares second-order polynomial curve. The resulting scaling parameter κ turns out to be identical.

Finally, we discuss the reasons for the disparities between the differing statistical scales. Among other factors, it is pointed out that the analyses of Zhang (1995) and Phillips (2002a) apply over limited (and differing) ranges of T_B, and assume a linear relation between T_B and R. It is therefore likely that the results of Phillips (2002a) are more accurate for lower temperature sources, whilst those of Zhang (1995) apply to outflows having $T_B > 1$ K – a range that includes the majority of known PNe.

REFERENCES

Acker A., 1978, A&AS, 33, 367
Acker A., Fresneau A., Pottasch S. R., Janiewicz G., 1998, A&A, 337, 253
Aller L. H., 1965, Landolt-Bornstein Tables, Group VI (Astronomy, Astrophysics, and Space Research). Springer-Verlag, Vienna
Bensby T., Lundstrom I., 2001, A&A, 374, 599
Blocker T., Schönberner D., 1990, A&A, 240, L11
Cahn J. H., Kaler J. B., Stanghellini L., 1992, A&AS, 94, 399
Ciardullo R., Bond H. E., Sipior M. S., Fullton L. K., Zhang C. Y., Schaefer K. G., 1999, AJ, 118, 488
Cudworth K. M., 1974, AJ, 79, 1384
Daub C. T., 1982, ApJ, 260, 612
Ferch R. L., Salpeter E. E., 1975, ApJ, 202, 195
Gathier R., Pottasch S. R., Pel J. W., 1986, A&A, 157, 171
Gutierrez-Moreno A., Anguita C., Loyola P., Moreno H., 1999, PASP, 111, 1163
Hajian A. R., Terzian Y., 1996, PASP, 108, 258
Hajian A. R., Terzian Y., Bignell C., 1993, AJ, 106, 1965
Harris H. C., Dahn C. C., Monet D. G., Pier J. R., 1997, in Habing H. J., Lamers H. J. G. L. M., eds, Proc. IAU Symp. 180, Planetary Nebulae. Kluwer Academic, Dordrecht, p. 40
Henry R. B. C., Shipman H. L., 1986, ApJ, 311, 774
Kaler J. B., Jacoby G. H., 1991, ApJ, 382, 134
Kaler J. H., Lutz J. B., 1983, PASP, 95, 739
Kwok S., 1985, ApJ, 290, 568
Liller M. H., Liller W., 1968, in Osterbrock D., O'Dell C. R., eds, Proc. IAU Symp. 34, Planetary Nebulae. Reidel, Dordrecht, p. 38
Maciel W. J., 2000, in Matteucci F., Giovanelli F., eds, The Evolution of the Milky Way: Stars Versus Clusters. Kluwer Academic, Dordrecht, p. 81
Maciel W. J., Pottasch S. R., 1980, A&A, 88, 1
Marigo P., Girardi L., Groenwegen M. A. T., Weiss A., 2001, A&A, 378, 958
Martin W., 1994, A&A, 281, 526
Mellema G., 1994, A&A, 290, 915
Mendez R. H., Niemela V. S., 1981, ApJ, 250, 240
Mendez R. H., Kudritzki R. P., Herrero A., Husfield D., Groth H. G., 1988, A&A, 190, 113
Mendez R. H., Kudritzki R. P., Herrero A., 1992, A&A, 260, 329
Minkowski R., Aller L. H., 1954, ApJ, 120, 261
Napiwotzki R., 2001, A&A, 367, 973
Napiwotzki R., Schönberner D., 1995, A&A, 301, 545
Okorokov V. A., Shustov B. M., Tutukov A. V., Yorke H. W., 1985, A&A, 142, 441
Phillips J. P., 2001, A&A, 367, 967
Phillips J. P., 2002a, ApJS, 139, 199
Phillips J. P., 2002b, A&A, 393, 1027
Phillips J. P., 2004, New Astron., 9, 391
Pottasch S. R., 1980, A&A, 89, 336
Pottasch S. R., 1996, A&A, 307, 561
Reed D. S., Balick B., Hajian A. R., Klayton T. L., Giovanardi S., Casertano S., Panagia N., Terzian Y., 1999, AJ, 118, 2430
Schmidt-Voigt M., Köppen J., 1987, A&A, 174, 211
Schneider S. E., Buckley D., 1996, ApJ, 459, 606
Schönberner D., 1979, A&A, 79, 108
Schönberner D., 1981, A&A, 103, 119
Schönberner D., 1983, ApJ, 272, 708
Schönberner D., 1989, in Torres-Peimbert S., ed., Proc. IAU Symp. 131, Planetary Nebulae. Kluwer Academic, Dordrecht, p. 464
Schönberner D., 1993, in Weinberger R., Acker A., eds, Proc. IAU Symp. 155, Planetary Nebulae. Kluwer Academic, Dordrecht, p. 415
Vassiliadis E., Wood P. R., 1994, ApJS, 92, 125
van de Steene G. C., Zijlstra A. A., 1994, A&A, 293, 541
Vorontsov-Veljaminov B. A., 1950, Astron. Zh., 27, 285
Weidemann V., 1989, A&A, 213, 155
Zhang C. Y., 1993, ApJ, 410, 239
Zhang C. Y., 1995, ApJS, 98, 659
Zhang C. Y., Kwok S., 1993, ApJS, 88, 137

APPENDIX A: RESULTS OF ALTERNATIVE (LOGARITHMIC) COMPARISON

There are various procedures one might use to investigate differences between independent sets of distances. A comparison between the mean distances of the sets, such as has been described in Section 4, has the merit of giving direct information concerning overall differences in *D*. It is also open to bias, however, and dominated by trends at larger values of *D*.

An alternative procedure would be to determine a mean logarithmic difference Γ between the various data sets, where

$$\Gamma = \frac{\sum_{i=1}^{N} \log[D_i(\mathrm{stat})/D_i(\mathrm{stand})]}{N}, \tag{A1}$$

and D_i(stand) and D_i(stat) are as described in Section 4. This parameter takes better account of trends at low and high values of *D*. It also possesses at least one further advantage. Most of the statistical distances are based upon trends within log–log planes. Thus, the variation of T_B with *R* is usually based upon the correlation between their respective logarithmic trends. It is therefore more appropriate, in comparing scales, to undertake an analysis of the logarithmic differences between their distances.

Such an analysis has been undertaken here for the eight statistical scales discussed in Section 4. The results are presented in Table A1, where we indicate both the values of Γ, and the modulus of the

Table A1. Summary of logarithmic scaling differences between statistical distance scales.

Comparative scale	Γ(all)	|Γ(all)|	Γ(low)	|Γ(low)|	Γ(high)	|Γ(high)|
Present work	+0.010 ± 0.022	0.218 ± 0.014	+0.009 ± 0.041	0.187 ± 0.022	+0.010 ± 0.025	0.224 ± 0.017
Zhang (1995)	+0.130 ± 0.024	0.262 ± 0.017	+0.382 ± 0.042	0.386 ± 0.040	+0.075 ± 0.026	0.234 ± 0.018
van de Steene & Zijlstra (1995)	+0.088 ± 0.023	0.244 ± 0.016	+0.294 ± 0.041	0.304 ± 0.039	+0.043 ± 0.026	0.231 ± 0.017
Phillips (2002a)	−0.306 ± 0.025	0.385 ± 0.017	−0.020 ± 0.042	0.191 ± 0.024	−0.369 ± 0.026	0.427 ± 0.019
Cahn et al. (1992)	−0.058 ± 0.025	0.267 ± 0.016	−0.157 ± 0.042	0.241 ± 0.026	−0.037 ± 0.029	0.273 ± 0.018
Daub (1982)	−0.176 ± 0.027	0.321 ± 0.017	−0.150 ± 0.042	0.238 ± 0.026	−0.181 ± 0.031	0.340 ± 0.020
Acker (1978)	−0.085 ± 0.031	0.260 ± 0.019	−0.102 ± 0.064	0.184 ± 0.039	−0.088 ± 0.033	0.269 ± 0.020
Bensby & Lundstrom (2001)	+0.134 ± 0.026	0.280 ± 0.018	+0.463 ± 0.043	0.464 ± 0.042	+0.062 ± 0.026	0.240 ± 0.018
Schneider & Buckley (1996)	−0.017 ± 0.024	0.236 ± 0.015	−0.233 ± 0.047	0.287 ± 0.036	+0.031 ± 0.025	0.224 ± 0.017

logarithmic distance

$$|\Gamma| = \frac{\sum_{i=1}^{N} |\log[D_i(\mathrm{stat})/D_i(\mathrm{stand})]|}{N}. \quad \text{(A2)}$$

The former parameter, Γ, gives an indication of biases in mean trends. If the comparative distances D_i(comp) are systematically lower or higher than is the case for D_i(stand), then this will show up as a positive or negative bias in Γ. The parameter |Γ|, by contrast, gives an indication of the spread (or dispersion) in the results.

As in Section 4, the parameters Γ and |Γ| have been determined for three ranges of brightness temperature. We give values for all of the sources combined (all), and also for sources having $\log(T_B) < -0.5$ (low) and $\log(T_B) \geqslant -0.5$ (high).

It may be seen that our present distances agree very closely indeed with those of the standard source distances, to levels that are even better than determined in Section 4. The differences in Γ are, in the mean, only of order 0.01 dex. This is, of course, not entirely surprising, as was discussed in our analysis in Section 4. It is also a very much better result than can be claimed for any other statistical scale.

All of the alternative scales have values of Γ that are significantly positive or negative, whether it be at high brightness temperatures, low brightness temperatures, or over both of these ranges together. This implies significant biases in all of the comparative statistical scales. The most extreme cases at low brightness temperatures are those of Zhang (1995) and Bensby & Lundstrom (2001), and it is obvious that neither of these scales is well suited to this particular range of T_B. Alternatively, the distances of Phillips (2002a) and Daub (1982) have strong negative values of Γ where T_B is large.

The present results therefore confirm the differences in scale noted in Section 4. They also emphasize, even more strongly than in the discussion of κ, that our present distances are applicable over the entire range of T_B.

This paper has been typeset from a TEX/LATEX file prepared by the author.